Accepted Manuscript

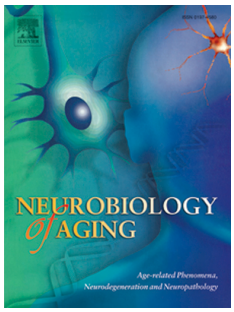

Traffic-related air pollution impact on mouse brain accelerates myelin and neuritic aging changes with specificity for CA1 neurons

N.C. Woodward, P. Pakbin, A. Saffari, F. Shirmohammadi, A. Haghani, C. Sioutas, M. Cacciottolo, T.E. Morgan, C.E. Finch

PII: S0197-4580(17)30008-8

DOI: 10.1016/j.neurobiolaging.2017.01.007

Reference: NBA 9821

To appear in: *Neurobiology of Aging*

Received Date: 11 August 2016

Revised Date: 16 November 2016

Accepted Date: 5 January 2017

Please cite this article as: Woodward, N., Pakbin, P, Saffari, A, Shirmohammadi, F, Haghani, A, Sioutas, C, Cacciottolo, M, Morgan, T., Finch, C., Traffic-related air pollution impact on mouse brain accelerates myelin and neuritic aging changes with specificity for CA1 neurons, *Neurobiology of Aging* (2017), doi: 10.1016/j.neurobiolaging.2017.01.007.

Traffic-related air pollution impact on mouse brain accelerates myelin and neuritic aging changes with specificity for CA1 neurons.

Woodward NC[1], Pakbin P[2], Saffari A[2], Shirmohammadi F[2], Haghani A[1], Sioutas C[2], Cacciottolo M[1], Morgan TE[1], Finch CE[1,3*].

1 Leonard Davis School of Gerontology, 2 Viterbi School of Engineering, 3 Dornsife College
University of Southern California, 3715 McClintock Ave Los Angeles, California, USA
*Corresponding author. Email cefinch@usc.edu.

Abstract 170/170 words:

Traffic-related air pollution (TRAP) is associated with lower cognition and reduced white matter volume in older adults, specifically for particulate matter <2.5 µm diameter ($PM_{2.5}$). Rodents exposed to TRAP have shown microglial activation and neuronal atrophy. We further investigated age differences of TRAP exposure, with focus on hippocampus for neuritic atrophy, white matter degeneration, and microglial activation. Young and middle-aged mice (3 and 18 month female C57BL/6J) were exposed to nanoscale-PM (nPM, <0.2 µm diameter). Young mice showed selective changes in the hippocampal CA1 region, with neurite atrophy (-25%), decreased MBP (-50%), and increased Iba1 (+50%), with dentate gyrus relatively unaffected. Exposure to nPM of young mice decreased GluA1 protein (-40%) and increased TNFa mRNA (10x). Older controls had age changes approximating nPM effects on young, with no response to nPM, suggesting an age ceiling effect. The CA1 selective vulnerability in young mice parallels CA1 vulnerability in Alzheimer's disease. We propose that TRAP associated human cognitive and white matter changes involve hippocampal responses to nPM that begin at younger ages.

Keywords: aging, white matter, air pollution, particulate matter, hippocampus, CA1

1. Introduction:

Traffic-related air pollution (TRAP) is a ubiquitous environmental toxin, which is associated with poorer cognitive performance in older populations (Power et al., 2011, Ranft et al., 2009, Wellenius et al., 2012, Zeng et al., 2010). The lower cognitive functioning approximates a two-year advance of normal cognitive decline from aging (Ailshire et al., 2014a, Ailshire et al., 2014b, Weuve et al., 2012). Brain structural and cellular changes are less documented. Small decreases of white matter (WM) volume were detected by MRI in older U.S. women of the Women's Health Initiative Memory Study (WHIMS) cohort who resided in zones of high level fine particulate matter ($PM_{2.5}$), with dose exposure in proportion to quartile $PM_{2.5}$ (Chen et al., 2015). Histochemical studies further showed WM microglial activation and blood brain barrier leakage in a small postmortem sample of young adults from a highly polluted Mexican city (Calderon et al., 2008, Calderon et al., 2011). In several rodent models, TRAP exposure activated microglia (Block et al., 2007, Block and Calderon, 2009, Cheng et al., 2016a). Effects of aging in animal models of TRAP have received limited study and show divergent age responses. Mumaw et al, 2016, reported increased cerebral cortex microglial reactivity with aging in male C57BL/6J mice ('B6') exposed to TRAP model *in vivo.*

In view of the potential importance of white matter loss from TRAP exposure in the WHIMS cohort (Chen et al., 2015), we examined the impact of aging on responses to TRAP in white matter and microglia of the dorsal hippocampus in female mice. Neuronal responses were included, because $PM_{2.5}$ exposure of B6 male mice caused selective atrophy of hippocampal CA1 pyramidal neurons (Fonken et al., 2011). The selectivity of CA1 neurons to TRAP is relevant to cognitive loss in association with $PM_{2.5}$, because the CA1 pyramidal neurons are the most vulnerable to Alzheimer's disease (AD) (Padurariu et al., 2012, Serrano-Pozo et al., 2011).

The present study addresses interactions of age and TRAP by chronically exposing young (3 month) and older (18 month) female B6 mice to nPM, a nano-size subfraction of ambient $PM_{2.5}$, which has greater cytotoxicity *in vivo* and *in vitro* than larger PM (Gillespie et al., 2013, Li et al., 2003). In neonatal neuron cultures nPM inhibited neurite outgrowth via TNFa and TNFR1, caused growth cone collapse (Cheng et al., 2016a). In hippocampal slice cultures nPM caused NMDA dependent neurotoxicity and nitrosylative stress, with both rescued by NMDA receptor antagonist AP5 (Morgan et al., 2011; Davis et al., 2013b).

The age of 18 m at tissue collection demographically approximates a paramenopausal group a decade or more earlier than in the WHIMS cohort. This age also minimizes pathological confounds from tumors and other senescent organ pathology which emerge after 22-24 months (Finch et al. 1969; Finch and Foster, 1971) in association with exponential increasing mortality (Finch and Pike, 1996).

2.1 Methods:

2.2 Animals and Ethics Statement:

C57BL/6J female mice, 3 and 18 m were obtained from the NIA Aging Mouse Colony, n=9 per group. Protocols were approved by the University of Southern California Institutional Animal Care and Use Committee, and animals were maintained under standard conditions according to NIH guidelines.

2.3 nPM Collection and Exposure:

Ambient nanoscale particulate matter (nPM; particles with aerodynamic diameters less than 0.18 μm) were collected on a 8 × 10 inch-Zeflour PTFE filters (Pall Life Sciences, Ann Arbor, MI) by a High-Volume Ultrafine Particle (HVUP) Sampler (Misra et al., 2002) at 400 L/min flow rate at the Particle Instrumentation Unit (PIU) of USC within 150 m downwind of a major freeway (I-110). These aerosols represent a mix of fresh ambient PM mostly from vehicular traffic on this freeway (Ning et al., 2007). Gravimetric mass (nPM mass concentration) was determined from pre- and post-weighing the filters under controlled temperature (22–24 ºC) and relative humidity (40–50%). The filter-deposited dried nPM were eluted by sonication into deionized water, yielding 340 μg/ml. Frozen stocks at 20 ℃ retain chemical stability for >30 days, including long-lived free radicals (Morgan et al., 2011, Li et al., 2003). Collected nPM has trace endotoxin levels (2.5 EU/mL, which equals approximately 0.3-0.6 ng/mL, by *Limulus* amoebocyte assay), equal to that eluted from filter collected ambient air. Endotoxin units at the concentration used for cell culture were 0.05-0.08 EU/mL, equivalent to sterile water.

Total elemental composition of the nPM samples was quantified by digestion of a section of the filter-collected nPM using a microwave aided, sealed bomb, mixed acid digestion (nitric acid, hydrofluoric acid and hydrochloric acid). Digests were subsequently analyzed by high resolution inductively coupled plasma sector field mass spectrometry (SF-ICPMS) (Herner et al., 2006).

Total nPM mass and number concentrations were 342 ± 49 μg/m^3 and 1.4 x 10^5 ± 9.7 x 10^3 particles/cm^3, respectively. The size distribution of the reaerosolized nPM was comparable to typical ambient aerosols, e.g. on the 710 Freeway (Ntziachristos et al., 2007). The chemical composition of ions (NH_4^+, NO_3^-, SO_4^{2-}) and water soluble organic compounds (WSOC) was similar to ambient air at the collection site (Morgan et al., 2011). The reaersolized nPM was depleted in insoluble species, including black carbon and polycyclic aromatic hydrocarbons. Figure 2 displays the average concentrations of inorganic elements in the nPM samples. Nineteen elements were >10 ng/m^3 (e.g., copper, Cu, 380 ng/m^3), and 29 elements were between 1-10 ng/m^3 (e.g., iron, Fe, 92.3 ng/m^3) (Figure 2A, B, respectively). The organic components of nPM are described in Morgan et al., 2011.

Mice were exposed 5 h/day, 3 d/week, for 10 weeks (Fig.1). Collected nPM was reaerosolized, mixed with HEPA filtered air, and delivered at a constant concentration. Control mice were exposed to only HEPA filtered air. The re-aerosolized nPM exposure stream was assayed for mass concentration by gravimetric analysis of filters parallel to the exposure stream before and after

each exposure. The number concentration of the inlet aerosol was monitored throughout the exposure period using a condensation particle counter (CPC, TSI Inc.). For the purpose of exposure, mice were transferred from home cages into sealed exposure chambers that allowed adequate ventilation and divided animals to minimize aggression, and returned to home cages immediately after exposure.

2.4 Weight and Behavior:

Weight: Mice were weighed before and throughout exposure. Statistical significance of age and nPM exposure effects was evaluated by 2-way repeated measures ANOVA and Bonferroni post-hoc test, and one-way ANOVA with Tukey post-hoc test at the end of exposure.

Novel Object Recognition (NOR): Short and long term memory were assessed by the NOR test. Mice were tested on a three-day protocol, to assess short and long term memory, and exploratory behavior. On day 1, mice were individually acclimatized to a dimly-lit black Plexiglas cubic box (20 x 20 x 20cm) for 15 min. After 24 h mice were returned to the box, and exposed to two identical novel objects (3.5 x 8 cm), which were affixed to the floor and placed symmetrically at 6 cm from the nearest walls. Mice were placed in a corner, facing the center and at equal distances from the two objects. Their start position was rotated and counterbalanced throughout the test. Exploration, defined as sniffing or touching of the two objects, was recorded; sitting on the object was not considered exploration. Ninety min. after the first trial, one object was replaced, and the procedure was repeated; 24 h later, the novel object was replaced with a second novel object, and the trial was repeated to assess long term memory. The novelty exploration index was calculated by time spent exploring the novel object, divided by time spent exploring the previous object. Statistical analysis for all tests used ANOVA, with Tukey's post-hoc test.

Spontaneous Alternation of Behavior (SAB): Working memory was assessed by the spontaneous alternation of behavior (SAB) test. The apparatus consisted of three equivalent arms (15 x 8 x 10 cm) made of black Plexiglas with equal angles between all arms. Mice were individually placed in one arm and allowed to freely explore for 10 min. The sequence and entries in each arm were recorded and percent alternation was determined from consecutive entries to the three different arms over the total number of transitions.

2.5 Histochemistry:

Dorsal hippocampus and forceps major of the corpus callosum paired with hippocampal alveus were analyzed by sagittal sections, approximately 1.80 mm from midline (Mouse Brain Atlas, Franklin and Paxinos, 3rd edition) for analysis of subregions CA1 stratum oriens (25 mm^2), CA1 stratum radiatum (45 mm^2), DG molecular layer (90 mm^2), and DG polymorphic layers (15 mm^2).

Immunofluorescence: Following cardiac saline perfusion, brain hemispheres were immersed in 4% paraformaldehyde overnight; cryoprotected in 30% sucrose; embedded in Optimal Cutting Temperature medium; and sliced sagittally in 18 µm thick sections on a cryostat. Sections were stored at -80 ℃. Tissue sections were permeabilized with 1% NP-40 and blocked with 5% bovine

serum albumin. Primary antibodies to Iba1 (ionized calcium binding adaptor molecule 1 (1:500, 019-19741, Wako Pure Chemical Industries, AB839504) or MBP (myelin basic protein, 1:1000, ab40390, Abcam, AB1141521) were added overnight at 4 ℃. Immunofluorescence was visualize d by Alex Fluor 488 and 594 antibodies (1:400, goat, Molecular Probes).

Silver Stain: Slides were defrosted, incubated in 20% silver nitrate for 15 min, followed by 20% silver nitrate for 15 min, before developing with a solution of formaldehyde, citric acid, nitric acid, and ammonium hydroxide (de Olmos et al., 1994). Slides were dehydrated and coverslipped with Permount.

Analysis: Using Image J, images were thresholded and quantified for total integrated density. Silver-stained images were analyzed to resolve cell bodies and processes. Results were normalized to the average of 3 m controls. Statistical analysis used ANOVA, with Tukey's post-hoc test.

2.6 Western Blots

Dorsal hippocampus of the contralateral hemisphere was microdissected and homogenized by a motor driven pestle on ice in 1x RIPA buffer (Millipore) supplemented with 1 mM PMSF, 1mM Na_3VO_2, 10 mM NaF, phosphatase inhibitor cocktail (Sigma), and Roche Complete Mini EDTA-free protease Inhibitor Cocktail Tablet (Roche). Homogenates were centrifuged 10,000 g x 10 min, and supernatants were analyzed by Western blot on Novex NuPAGE 4-12% Bis-Tris protein gels (Thermo Scientific). Membranes were washed with phosphate buffered saline with 0.05% tween-20, and blocked with 5% BSA for 1 hour at room temperature. Primary incubation was overnight at 4℃ for glutamatergic receptor protein subunits GluA1 (Abcam), GluA2 (Millipore), NR2A (Millipore), NR2B (Millipore), and other synaptic proteins (Sigma) at 1:1,000 overnight, and followed by secondary antibodies (1:10,000) conjugated with IRDye 800 (mouse, LI-COR Biosciences) or IRDye 680 (rabbit, LI-COR Biosciences) for 1 hour. Protein bands were quantified by Qdyssey V3.0 software (LI-COR Biosciences).

2.7 q-PCR

Hippocampal tissue was microdissected and homogenized by motor driven pestle in TriReagent (Sigma) and 1-bromo-3-chloropropane (Sigma). cDNA was reverse transcribed (Promega) for q-PCR with Taq Master Mix (Biopioneer). Primers used were *TNFa* (Forward: CGTCAGCCGATTTGCTATCT; Reverse: CGGACTCCGCAAAGTCTAAG), *TNFR1* (Forward: TGCCTCTGGTTATCTTCCTA; Reverse: GGGGCTTAGTAACAATTCCT), and *GAPDH* (Forward: CCAATGTGTCCGTCGTGGATCT; Reverse: GTTGAAGTCGCAGGAGACAACC). Q-PCR was quantified by delta-delta-CT.

3. Results:

Female C57BL/6J mice of specified ages were exposed to 150 hours of nPM during 10 weeks. Mice were behaviorally tested before analysis of brains by histochemistry and for protein and RNA.

3.1 Histochemistry

The dorsal hippocampus and corpus callosum, including the alveus, were examined for neuronal morphological changes, white matter myelin basic protein (MBP), and microglial activation. Figure 3 show illustrative images. Age differences are summarized in Table 1; nPM responses of the young, Table 2. The mouse age is shown at the beginning of the 10 week exposure.

Neurites: Silver staining of neurites showed effects of age and nPM, with no change in perikarya. Controls showed 25% decrease in CA1 neurite area with age (18 m vs 3 m), whereas dentate gyrus (DG) neurites did not show age change (Figure 4, ANOVA $p<0.05$). For nPM exposure, only the young mice responded, with 25% fewer neuritic processes in the CA1 stratum oriens and stratum radiatum (Figure 4A, B, ANOVA $p<0.05$). nPM had no effect on CA3 or DG neurite areas in either age group (Figure 4C, D). Perikaryal staining did not change with age or exposure in these regions (Supplementary Figure 1).

White Matter: In controls, myelin basic protein (MBP) was decreased in older mice in CA1 stratum oriens (-50%), and the DG polymorphic layer (-45%) (Figure 5A, C, ANOVA $p<0.05$). For nPM exposure, only young mice responded, with 50% decreased MBP in the CA1 stratum oriens (Figure 5A, ANOVA $p<0.05$). Exposure did not alter polymorphic or molecular layers of the DG (Figure 5C, D), or corpus callosum (forceps major) and hippocampal alveus (Figure 5E). Older nPM exposed mice showed no further decrease in MBP.

Microglial Activation: Iba1 immunostaining, a marker for microglial activation, showed +35% age increase in controls (Figure 6A, $p<0.05$, 2-tailed t-test). nPM exposure increased Iba1 in young mice by +50% in CA1 stratum oriens (Figure 6A; ANOVA $p<0.05$), and by +50% in DG polymorphic layer (Figure 6C, ANOVA $p<0.05$). Exposure to nPM did not alter Iba1 in CA1 stratum radiatum, DG molecular layer, corpus callosum and alveus (Figure 6B, D, E).

3.2 Protein and RNA by Western Blot and q-PCR

Glutamatergic receptor protein subunits in whole hippocampal extracts showed selective changes by Western blots. We focused on AMPA receptors (GluA1 and GluA2), which were selectively vulnerable to nPM in young male mice whereas NMDA subunits were not affected (Morgan et al. 2011). In non-exposed controls, GluA1 protein was decreased -50% by age alone (Figure 7A, ANOVA $p<0.05$). Only young mice responded to nPM with -50% decrease in GluA1. Cortical GluA1 protein did not differ by age. Three other subunits did not differ by age or respond to nPM: GluR2, NR2A, NR2B (Figure 7B,C,D). No change was observed in phosphorylation of GluA1 at S845 or S831, or of NR2B at S1303 by age or nPM.

TNFa mRNA responded to nPM with major 10-fold increase in young mice (Figure 7A). Older mice had highly variable TNFa which reduced significance of

possible age increase (Figure 7E, t-test p=0.002). TNFR1 mRNA showed no change by age or treatment (Figure 7F).

3.3 Body Weight and Behavior

Body weight: All groups lost weight during the first three weeks of exposure (Figure 8; p<0.01, 2-way ANOVA), presumably due to handling and noise stress. Young control and exposed mice, as well as older controls, regained their initial weight by the end of the 10-week exposure. In contrast, older mice did not recover weight loss during the exposure (Figure 8; one-way ANOVA, p<0.05), but by 4 weeks after exposure had regained the lost weight. Young mice, both nPM and control, which maintained weight throughout exposure, gained weight after conclusion of the exposure (Figure 8; two-way ANOVA, p<0.0001).

Cognition and Activity: No memory deficits were observed for age or for nPM exposure by NOR (Figure 9B) or SAB (Figure 10B). However, nPM exposure did decrease exploratory activity in both tests. The novel object recognition (NOR) test for short- and long-term memory showed 30% less exploration for older mice exposed to nPM vs controls (Figure 9A; ANOVA p<0.01). In the spontaneous alternation of behavior (SAB) test for short-term memory, the total arm entries were decreased in both young and older mice, vs age matched controls (Figure 10A, two-way ANOVA, p<0.05). Individual weight loss was correlated with locomotor activity change for older exposed mice (Figure 11; r=0.51), with the heavier exploring more.

4. Discussion

Young female mice (3 m) given 10 weeks of intermittent exposure to nPM from ambient urban traffic emissions showed changes resembling baseline aging changes of hippocampal CA1 subregion-specific decrease of MBP in WM and atrophy of CA1 neurites, together with microglial activation. Young nPM exposed mice also showed decreased hippocampus GluA1 protein and increased TNFa mRNA.

The reduction in myelin basic protein (MBP) is the first experimental evidence of WM alteration by air pollution exposure. These findings extend observed correlations of WM volume loss with ambient PM2.5 in older woman of the WHIMS cohort (Chen et al., 2016), which could be in part responsible for the decline in cognitive performance from TRAP exposure in older populations (Ranft et al., 2009, Wellenius et al., 2012, Zeng et al., 2010), approximating two-years of normal cognitive aging (Ailshire et al., 2014a, Ailshire et al., 2014b). This change could begin at young ages, evidenced from WM microglial activation in a small postmortem sample from a highly polluted Mexican city (Calderon et al., 2008, Calderon et al., 2011). Future studies will analyze WM for MBP isoforms and other WM proteins, as well as fiber density.

4.1 Aging and response to nPM

Responses to nPM were diminished by aging. In young adult mice, the nPM exposure decreased MBP levels and neurites, and increased microglial

activation in the hippocampal CA1 subfields. The older controls (non-exposed, 18 m.), had 25% lower CA1 neurite density and 50% less MBP, with a trend toward microglial activation. Older controls also showed decreased GluA1 and increased TNFa. However, the older mice did not respond to nPM with further atrophic brain changes. The diminished response of older mice to nPM were anticipated by the smaller kainate excitotoxic lesions of 20 and 24 m old aging male rats vs 3 m (Kesslak et al., 1995). The mechanisms behind the age-ceiling effect of hippocampus to nPM could involve an age-related loss of glutamate receptors (Figure 7A; Magnussen and Cotman, 1993) and age-related insensitivity to excitotoxins in the CA1 (Kerr et al., 2002), reported for older male rats. Our results support this hypothesis, with baseline decreased GluA1 in older mice. These findings also extend findings that 18 m old male C57BL/6J mice did not respond to nPM with induction of phase II electrophile responses in cerebellum, lung, and liver (Zhang et al., 2012).

Older mice showed nPM vulnerability in weight loss and behavioral activity. Older exposed mice lost more body weight during nPM exposure, and unlike the young and the older controls, did not recover weight until 1 month post exposure. Older nPM exposed mice also had reduced exploration in the novel object recognition test (30% reduction). Both young and older exposed mice showed less alternations in the SAB test (20% reduction). Moreover, individual weight loss was correlated with locomotor activity change for older exposed mice, with heavier animals exploring more.

The tests of short-term and long-term memory did not show effects of age or nPM. The novel object recognition (NOR) test measures declarative memory, but does not specifically resolve pattern completion. Memory tests that delineate between mechanisms of recall (Fanselow 1990; Matus-Amat et al., 2004) could be considered in future studies. Because the NOR is not directly hippocampal dependent, future studies could include contextual object recognition tests which are hippocampal dependent, e.g. Novel Object In Context (NOIC (Balderas et al., 2008). A comprehensive brain regional analysis is needed to identify the vulnerability of neuronal pathways to ambient pollutants across the lifespan. This effort is justified by the global impact of air pollution on health and mortality, which the WHO ranks in top 20 leading risk factors for mortality (WHO 2009).

4.2 Young mice nPM responses

Contrary to the absence of nPM effects on memory, we found CA1-specifc neurite atrophy in young mice. The regional vulnerability of hippocampal neurons gives a precedent for further inquiry. The CA1 stratum oriens responded most to nPM exposure, with an 25% neurite atrophy, 50% reduction in MBP, and 50% increase in Iba1. The stratum radiatum showed changes only in neurites, while white matter and Iba1 remaining unchanged. These regions, though adjacent, differ in vascularization, cell population, and connectivity, which could explain the divergent responses to nPM. The stratum oriens is more densely vascularized than the stratum radiatum (Duvernoy et al., 2013, Grivas et al., 2003) and has different connectivity. For example, the entorhinal cortex projections to the stratum oriens are denser than to the stratum radiatum, while CA3 sends

projections to both strata, but with more projections to the radiatum, via the Schaffer collaterals (Figure 2E). The MBP and microglial changes in response to nPM were observed only in the stratum oriens, which predicts LTP impairments to nPM in the oriens.

The selective atrophy of CA1 neurites in young C57BL/6J female mice in our study confirms the Golgi analysis of Fonken et al., 2011, for young male B6 mice; in both studies the DG neurites were unchanged. The silver staining of 18 um sections could not resolve dendritic spines or other neuronal subprocesses. The differential CA1 vulnerability to two models of TRAP exposure closely matches the CA1 vulnerability in AD, wherein the CA1 neurons undergo earlier and greater degeneration than the DG (Padurariu et al., 2012, Serrano-Pozo et al., 2011). This regional vulnerability has important implications for the cognitive consequences of TRAP exposure. The CA1 is integral in spatial memory (Tsien et al., 1996), consistent with the poorer performance on the Barnes maze of $PM_{2.5}$ exposed mice (Fonken et al., 2011). The CA1 also mediates object recognition, specifically pattern completion recall, based on familiar cues, and is mediated by the CA3/CA1 pathway (Leal and Yassa, 2015).

Effect of nPM on glutamate receptors in young mice was selective to GluA1 AMPA receptors, with no change in GluA2, or the NMDA receptors NR2A and NR2B. This selectivity was observed in male mice with the same nPM exposure (Morgan et al., 2011). Neonatal hippocampal slice experiments also show acute glutamatergic pathway responses to nPM: the greater CA1 vulnerability and induction of NO and nitrosylation were attenuated by the NMDA receptor antagonist AP5 (Davis et al., 2013b).

The neurite atrophy with decreased length could be TNFa dependent. *In vitro* nPM exposure reduced neurite outgrowth in a TNFa/TNFR1 dependent manner (Cheng et al., 2016a). Hippocampal TNFa mRNA was increased 10x in by nPM exposure in the present studies. *In vitro* blocking TNFa by siRNA or immunoneutralization was able to rescue neurite growth, as was blocking TNFR1 by anti-TNFR1 peptide (Cheng et al., 2016a). We saw no change in TNFR1 mRNA, corroborating findings on the olfactory neuroepithelium (Cheng et al., 2016a).

4.3 Exposure Composition

The exposure concentrations used here are roughly equal in overall particle numbers to ambient on-road concentrations (Ntziachristos et al., 2007). The overall delivered dose over the 10-week exposure protocol is roughly equivalent to one year of human exposure to freeway levels of nPM. The nPM used here is generalizable to other cities, as it is mostly derived from automobile traffic. Despite the overall low levels of metals in ambient nPM, redox-active elements such as Cu, Cr, Fe, Mn and Ni have been attributed to adverse health outcomes (Molinelli et al., 2002; Oller 2002; Wise et al., 2002). Prior studies in the Los Angeles basin and elsewhere have indicated that these metals in the sub-micron size ranges are mostly emitted from motor vehicles, including tailpipe emissions, brake wear, tire wear, and re-suspended road dust, in addition to combustion products (Schauer et al., 2006; Saffari et al., 2013).

4.4 Potential Mechanisms

The transport of nPM and other TRAP components into the brain is unresolved and includes at least two routes, 'nose-to-brain' and 'lung-to-brain'. Other ultrafine PM (radiolabelled carbon and manganese) can be translocated to the brain from the olfactory neurons in the nasal epithelium into the olfactory bulb, but also to other brain regions (Oberdorster et al., 2004, Elder et al., 2006), We recently showed rapid inflammatory responses in the olfactory bulb to inhaled nPM (Cheng et al. 2016a). Additionally, Mumaw et al., 2016, showed evidence for a lung-to-brain route in responses to ozone which did not involve TNFa or other cytokines. Nonetheless, TRAP exposure can increase blood TNFa in humans (Delfino et al., 2009) and mice (Li et al. 2013, van Eeden et al., 2001). Elucidating specific chemical mechanisms in responses to nPM and other TRAP components is complicated by their extreme chemical heterogeneity (Morgan et al., 2011; Liu et al., 2016). Besides direct 'nose-to-brain' passage of inhaled air particulates, radiolabeled ultrafine carbon PM rapidly reached the cerebellum at about the same time as the olfactory bulb (Oberdorster et al., 2004), suggesting other routes into the brain. The possibility of systemic effects of inhaled TRAP are consistent with the broad brain regional responses to TRAP inhalation, which include cerebellum (Cheng et al., 2016; Zhang et al., 2012) and other regions that are multiple synapses away from olfactory input.

The cellular mechanisms of nPM induced neurodegeneration could be mediated by chronic microglial activation, which produces both extracellular reactive oxygen species and neurotoxic factors (Block et al., 2007, Mumaw et al., 2016, Davis et al., 2013b). LPS based microglial activation shows neuronal loss in microglial rich brain regions (Qin et al., 2007), and causes reduced neuronal processes in the CA1 (Richwine et al., 2008). Exposure to nPM shows neuroinflammatory effects including induced inflammatory cytokines seen in the cerebral cortex (Morgan et al., 2011), and increased phase II response genes in the cerebellum (Zhang et al., 2012). nPM treatment of mixed glial cultures increased IL-1a and TNFa with dose dependence (Morgan et al., 2011). The current study extends these results of neuroinflammation in the CA1 and dentate gyrus, and subregional specificity of the nPM response.

5. Conclusion:

Shown here, nPM leads to hippocampal neurite atrophy and decreased white matter MBP. The regional specificity to the CA1 predicts a degradation of CA1 functions in human populations exposed to high levels of air pollution, which underlie accelerated cognitive impairments. Future imaging studies of WHIMS and other well defined cohorts may resolve earlier stages of neurodegenerative responses to TRAP and their relationship to AD risk.

Acknowledgements: We thank Prof. Joshua Millstein for statistical advice; and Prof. Jiu Chiuan Chen for his careful review of the manuscript. This work was

supported by the National Institutes of Aging (T32AG0037, R21 AG-040753, R21 AG-050201).

Bibliography:

Ailshire JA, Clarke P. Fine particulate matter air pollution and cognitive function among U.S. older adults. J Gerontol B Psychol Sci Soc Sci. 2015 Mar;70(2):322-8. doi: 10.1093/geronb/gbu064.

Ailshire JA, Crimmins EM. Fine particulate matter air pollution and cognitive function among older US adults. Am J Epidemiol. 2014 Aug 15;180(4):359-66. doi: 10.1093/aje/kwu155.

Balderas I, Rodriguez-Ortiz CJ, Salgado-Tonda P, Chavez-Hurtado J, McGaugh JL, Bermudez-Rattoni F. The consolidation of object and context recognition memory involve different regions of the temporal lobe. Learn Mem. 2008 Aug 21;15(9):618-24. doi: 10.1101/lm.1028008. PubMed PMID: 18723431; PubMed Central PMCID: PMC2632790

Block ML, Zecca L, Hong JS. Microglia-mediated neurotoxicity: uncovering the molecular mechanisms. Nat Rev Neurosci. 2007 Jan;8(1):57-69.

Block ML, Calderón-Garcidueñas L. Air pollution: mechanisms of neuroinflammation and CNS disease. Trends Neurosci. 2009 Sep;32(9):506-16. doi: 10.1016/j.tins.2009.05.009.

Bolton JL, Smith SH, Huff NC, Gilmour MI, Foster WM, Auten RL, Bilbo SD. Prenatal air pollution exposure induces neuroinflammation and predisposes offspring to weight gain in adulthood in a sex-specific manner. FASEB J. 2012 Nov;26(11):4743-54. doi: 10.1096/fj.12-210989.

Calderón-Garcidueñas L, Solt AC, Henríquez-Roldán C, Torres-Jardón R, Nuse B, Herritt L, Villarreal-Calderón R, Osnaya N, Stone I, García R, Brooks DM, González-Maciel A, Reynoso-Robles R, Delgado-Chávez R, Reed W. Long-term air pollution exposure is associated with neuroinflammation, an altered innate immune response, disruption of the blood-brain barrier, ultrafine particulate deposition, and accumulation of amyloid beta-42 and alpha-synuclein in children and young adults. Toxicol Pathol. 2008 Feb;36(2):289-310. doi: 10.1177/0192623307313011.

Calderón-Garcidueñas L, Engle R, Mora-Tiscareño A, Styner M, Gómez-Garza G, Zhu H, Jewells V, Torres-Jardón R, Romero L, Monroy-Acosta ME, Bryant C, González-González LO, Medina-Cortina H, D'Angiulli A. Exposure to severe urban air pollution influences cognitive outcomes, brain volume and systemic inflammation in clinically healthy children. Brain Cogn. 2011 Dec;77(3):345-55. doi: 10.1016/j.bandc.2011.09.006.

Chen JC, Wang X, Wellenius GA, Serre ML, Driscoll I, Casanova R, McArdle JJ, Manson JE, Chui HC, Espeland MA. Ambient air pollution and neurotoxicity on brain structure: Evidence from women's health initiative memory study. Ann Neurol. 2015 Sep;78(3):466-76. doi: 10.1002/ana.24460.

Cheng H, Saffari A, Sioutas C, Forman HJ, Morgan TE, Finch CE. Nano-Scale Particulate Matter from Urban Traffic Rapidly Induces Oxidative Stress and Inflammation in Olfactory Epithelium with Concomitant Effects on Brain. Environ Health Perspect. 2016 May 17.

Conrad CD. Chronic Stress-Induced Hippocampal Vulnerability: The Glucocorticoid Vulnerability Hypothesis. Reviews in the neurosciences. 2008;19(6):395-411.

Davis DA, Bortolato M, Godar SC, Sander TK, Iwata N, Pakbin P, Shih JC, Berhane K, McConnell R, Sioutas C, Finch CE, Morgan TE. Prenatal exposure to urban air nanoparticles in mice causes altered neuronal differentiation and depression-like responses. PLoS One. 2013 May 29;8(5):e64128. doi: 10.1371/journal.pone.0064128.

Davis DA, Akopian G, Walsh JP, Sioutas C, Morgan TE, Finch CE. Urban air pollutants reduce synaptic function of CA1 neurons via an NMDA/NȮ pathway in vitro. J Neurochem. 2013 Nov;127(4):509-19. doi: 10.1111/jnc.12395.

de Olmos JS, Beltramino CA, de Olmos de Lorenzo S. Use of an amino-cupric-silver technique for the detection of early and semiacute neuronal degeneration caused by neurotoxicants, hypoxia, and physical trauma. Neurotoxicology and teratology 1994; 16(6): 545-561.

Delfino RJ, Staimer N, Tjoa T, Gillen DL, Polidori A, Arhami M, Kleinman MT, Vaziri ND, Longhurst J, Sioutas C. Air pollution exposures and circulating biomarkers of effect in a susceptible population: clues to potential causal component mixtures and mechanisms. Environ Health Perspect. 2009 Aug;117(8):1232-8. doi: 10.1289/ehp.0800194.

Driscoll I, Hamilton DA, Petropoulos H, Yeo RA, Brooks WM, Baumgartner RN, Sutherland RJ. The aging hippocampus: cognitive, biochemical and structural findings. Cereb Cortex. 2003 Dec;13(12):1344-51.

Duvernoy, Henri M., Cattin, Francoise, Risold, Pierre-Yves
Duvernoy HM, Cattin F, Risold P. The Human Hippocampus- Functional Anatomy, Vascularization, and Serial Sections with MRI. Springer. 2013

Elder A, Gelein R, Silva V, Feikert T, Opanashuk L, Carter J, Potter R, Maynard A, Ito Y, Finkelstein J, Oberdörster G.Translocation of inhaled ultrafine

manganese oxide particles to the central nervous system. Environ Health Perspect. 2006 Aug;114(8):1172-8. Erratum in: Environ Health Perspect. 2006 Aug;114(8):1178.

Fanselow, M. S. (1990). Factors governing one-trial contextual conditioning. Animal Learning & Behavior, 18(3), 264–270. doi:10.3758/bf03205285

Finch CE. The neurobiology of middle-age has arrived. Neurobiol Aging. 2009 Apr;30(4):515-20; discussion 530-33. doi: 10.1016/j.neurobiolaging.2008.11.011.

Finch CE, Foster JR. Hematologic and serum electrolyte values of the C57BL-6J male mouse in maturity and senescence. Lab Anim Sci. 1973 Jun;23(3):339-49.

Finch CE, Pike MC. Maximum life span predictions from the Gompertz mortality model. J Gerontol A Biol Sci Med Sci. 1996; 51(3):B183–B194.

Fonken, L. K., Xu, X., Weil, Z. M., Chen, G., Sun, Q., Rajagopalan, S., & Nelson, R. J. (2011). Air pollution impairs cognition, provokes depressive-like behaviors and alters hippocampal cytokine expression and morphology. Mol Psychiatry, 16(10), 987–995. doi:10.1038/mp.2011.76

Gillespie P, Tajuba J, Lippmann M, Chen LC, Veronesi B. Particulate matter neurotoxicity in culture is size-dependent. Neurotoxicology. 2013 May;36:112-7. doi: 10.1016/j.neuro.2011.10.006.

Grivas I, Michaloudi H, Batzios Ch, Chiotelli M, Papatheodoropoulos C, Kostopoulos G, Papadopoulos GC. Vascular network of the rat hippocampus is not homogeneous along the septotemporal axis. Brain Res. 2003 May 9;971(2):245-9.

Herner, J.D., Green, P.G., Kleeman, M.J., 2006. Measuring the Trace Elemental Composition of Size-Resolved Airborne Particles. Environ. Sci. Technol. 40, 1925–1933. doi:10.1021/es052315q

Hesp BR, Wrightson T, Mullaney I, Kerr DS. Kainate receptor agonists and antagonists mediate tolerance to kainic acid and reduce high-affinity GTPase activity in young, but not aged, rat hippocampus. J Neurochem. 2004 Jul;90(1):70-9.

Kerr DS, Razak A, Crawford N. Age-related changes in tolerance to the marine algal excitotoxin domoic acid. Neuropharmacology. 2002 Sep;43(3):357-66.

Kesslak JP, Yuan D, Neeper S, Cotman CW. Vulnerability of the hippocampus to kainate excitotoxicity in the aged, mature and young adult rat. Neurosci Lett. 1995 Mar 24;188(2):117-20.

583 Kunstyr I, Leuenberger HG. Gerontological data of C57BL/6J mice. I. Sex
584 differences in survival curves. J Gerontol. 1975 Mar;30(2):157-62.
585
586 Leal, S. L., & Yassa, M. A. (2015). Neurocognitive Aging and the Hippocampus
587 across Species. Trends in Neurosciences, 38(12), 800–812.
588 doi:10.1016/j.tins.2015.10.003
589
590 Li N, Sioutas C, Cho A, Schmitz D, Misra C, Sempf J, Wang M, Oberley T,
591 Froines J, Nel A. Ultrafine particulate pollutants induce oxidative stress and
592 mitochondrial damage. Environ Health Perspect. 2003 Apr;111(4):455-60.
593
594 Li R, Navab M, Pakbin P, Ning Z, Navab K, Hough G, Morgan TE, Finch CE,
595 Araujo JA, Fogelman AM, Sioutas C, Hsiai T. Ambient ultrafine particles alter
596 lipid metabolism and HDL anti-oxidant capacity in LDLR-null mice. J Lipid Res.
597 2013 Jun;54(6):1608-15. doi: 10.1194/jlr.M035014.
598
599 Liu Q, Babadjouni R, Radwanski R, Cheng H, Patel A, Hodis DM, He S,
600 Baumbacher P, Russin JJ, Morgan TE, Sioutas C, Finch CE, Mack WJ. Stroke
601 Damage Is Exacerbated by Nano-Size Particulate Matter in a Mouse
602 Model. PLoS One. 2016 Apr 12;11(4):e0153376. doi:
603 10.1371/journal.pone.0153376.
604
605 Magnusson KR, Cotman CW. Age-related changes in excitatory amino acid
606 receptors in two mouse strains. Neurobiol Aging. 1993 May-Jun;14(3):197-206.
607
608 Matus-Amat P, Higgins EA, Barrientos RM, Rudy JW. The role of the dorsal
609 hippocampus in the acquisition and retrieval of context memory
610 representations. J Neurosci. 2004 Mar 10;24(10):2431-9.
611
612 Misra C, Kim S, Shen S, Sioutas C. A high flow rate, very low pressure drop
613 impactor for inertial separation of ultrafine from accumulation mode particles. J
614 Aerosol Sci. 2002; 33:735-752
615
616 Molinelli, A.R., Madden, M.C., McGee, J.K., Stonehuerner, J.G., Ghio, A.J. 2002.
617 Effect of metal removal on the toxicity of airborne particulate matter from the
618 Utah Valley. Inhalation Toxicol 14:1069–1086.
619
620 Morgan TE, Davis DA, Iwata N, Tanner JA, Snyder D, Ning Z, Kam W, Hsu YT,
621 Winkler JW, Chen JC, Petasis NA, Baudry M, Sioutas C, Finch
622 CE. Glutamatergic neurons in rodent models respond to nanoscale particulate
623 urban air pollutants in vivo and in vitro. Environ Health Perspect. 2011
624 Jul;119(7):1003-9. doi: 10.1289/ehp.1002973.
625
626 Ning Z, Geller MD, Moore KF, Sheesley R, Schauer JJ, Sioutas C. Daily variation
627 in chemical characteristics of urban ultrafine aerosols and inference of their
628 sources. Environ Sci Technol. 2007 Sep 1;41(17):6000-6.

Ntziachristos L, Ning Z, Geller MD, Sioutas C. Particle concentration and Characteristics near a major freeway with heavy-duty diesel traffic. Environ Sci Technol. 2007 Apr 1;41(7):2223-30. PubMed PMID: 17438767.

Oberdörster G, Sharp Z, Atudorei V. Translocation of inhaled ultrafine particles to the brain. Inhal Toxicol. 2004; 16: 437-445.

Oller, A.R. 2002. Respiratory carcinogenicity assessment of soluble nickel compounds. Environ Health Perspect 110(Suppl 5):841–844.

Padurariu M, Ciobica A, Mavroudis I, Fotiou D, Baloyannis S. Hippocampal neuronal loss in the CA1 and CA3 areas of Alzheimer's disease patients. Psychiatr Danub. 2012 Jun;24(2):152-8.

Power MC, Weisskopf MG, Alexeeff SE, Coull BA, Spiro A 3rd, Schwartz J. Traffic-related air pollution and cognitive function in a cohort of older men. Environ Health Perspect. 2011 May;119(5):682-7. doi: 10.1289/ehp.1002767.

Qin L, Wu X, Block ML, Liu Y, Breese GR, Hong JS, Knapp DJ, Crews FT. Systemic LPS causes chronic neuroinflammation and progressive neurodegeneration. Glia. 2007 Apr 1;55(5):453-62.

Ranft U, Schikowski T, Sugiri D, Krutmann J, Krämer U. Long-term exposure to traffic-related particulate matter impairs cognitive function in the elderly. Environ Res. 2009 Nov;109(8):1004-11. doi: 10.1016/j.envres.2009.08.003.

Richwine AF, Parkin AO, Buchanan JB, Chen J, Markham JA, Juraska JM, Johnson RW. Architectural changes to CA1 pyramidal neurons in adult and aged mice after peripheral immune stimulation. Psychoneuroendocrinology. 2008 Nov;33(10):1369-77. doi: 10.1016/j.psyneuen.2008.08.003.

Saffari, A., Daher, N., Shafer, M.M., Schauer, J.J., Sioutas, C., 2013. Seasonal and spatial variation of trace elements and metals in quasi-ultrafine (PM0.25) particles in the Los Angeles metropolitan area and characterization of their sources. Environ. Pollut. 181, 14–23. doi:10.1016/j.envpol.2013.06.001

Schauer, J.J., Lough, G.C., Shafer, M.M., Christensen, W.F., Arndt, M. F., DeMinter, J.T., Park, J. S. 2006. Characterization of Metals Emitted from Motor Vehicles Res. Rep.-Health Eff. Inst., 1–76, discussion 77–88

Serrano-Pozo A, Frosch MP, Masliah E, Hyman BT. Neuropathological Alterations in Alzheimer Disease. Cold Spring Harbor Perspectives in Medicine:2011;1(1):a006189. doi:10.1101/cshperspect.a006189.

Tsien JZ, Huerta PT, Tonegawa S. The essential role of hippocampal CA1 NMDA receptor-dependent synaptic plasticity in spatial memory. Cell. 1996 Dec 27;87(7):1327-38.

van Eeden SF, Tan WC, Suwa T, Mukae H, Terashima T, Fujii T, Qui D, Vincent R, Hogg JC. Cytokines involved in the systemic inflammatory response induced by exposure to particulate matter air pollutants (PM(10)). Am J Respir Crit Care Med. 2001 Sep 1;164(5):826-30.

Wang Y, Eliot MN, Kuchel GA, Schwartz J, Coull BA, Mittleman MA, Lipsitz LA, Wellenius GA. Long-term exposure to ambient air pollution and serum leptin in older adults: results from the MOBILIZE Boston study. J Occup Environ Med. 2014 Sep;56(9):e73-7. doi: 10.1097/JOM.0000000000000253.

Wellenius GA, Boyle LD, Coull BA, Milberg WP, Gryparis A, Schwartz J, Mittleman MA, Lipsitz LA. Residential proximity to nearest major roadway and cognitive function in community-dwelling seniors: results from the MOBILIZE Boston Study. J Am Geriatr Soc. 2012 Nov;60(11):2075-80. doi: 10.1111/j.1532-5415.2012.04195.x.

Weuve J, Puett RC, Schwartz J, Yanosky JD, Laden F, Grodstein F. Exposure to particulate air pollution and cognitive decline in older women. Arch Intern Med. 2012 Feb 13;172(3):219-27. doi: 10.1001/archinternmed.2011.683.

WHO (2009). Global health risks: Mortality and burden of diseases attributable to selected major risks. Geneva, World Health Organization (http://www.who.int/healthinfo/global_burden_disease/GlobalHealthRisks_report_full.pdf).

Wise, J.P. Sr, Wise, S.S., Little, J.E. 2002. The cytotoxicity and genotoxicity of particulate and soluble hexavalent chromium in human lung cells. Mutat Res 517:221–229.

Zeng Y, Gu D, Purser J, Hoenig H, Christakis N. Associations of environmental factors with elderly health and mortality in China.Am J Public Health. 2010 Feb;100(2):298-305. doi: 10.2105/AJPH.2008.154971.

Zhang H, Liu H, Davies KJ, Sioutas C, Finch CE, Morgan TE, Forman HJ. Nrf2-regulated phase II enzymes are induced by chronic ambient nanoparticle exposure in young mice with age-related impairments. Free Radic Biol Med. 2012 May 1;52(9):2038-46. doi: 10.1016/j.freeradbiomed.2012.02.042.

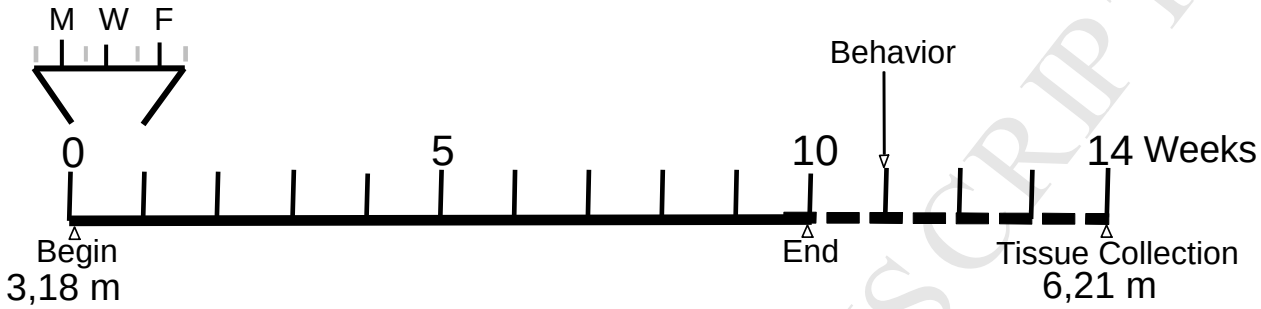

Figure 1: Experimental exposure schedule, showing expanded alternate day intermittent exposure schedule for the initial week; ages of mice at beginning and end of experiment below the timeline.

744

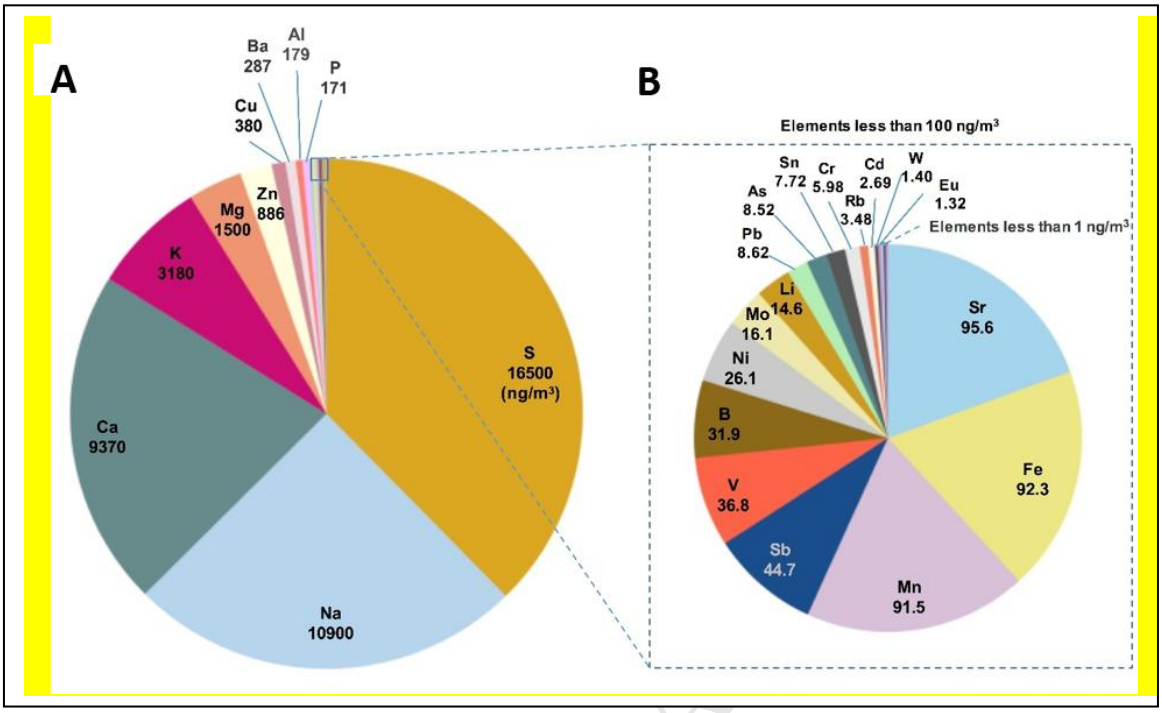

745

746 **Figure 2**: Composition of reaersolized nPM used for exposures. Mass
747 concentration, 342 ± 81 µg/m^3; particle number concentration, $1.4\times10^5 \pm 9.7\times10^3$
748 particles /cm^3. Top inorganic elements are listed in ng/m^3. A, Top 10 elements by
749 concentration. B, Expanded scale for remaining elements with a concentration
750 >1.0 ug/m^3.

751
752
753
754
755
756
757
758

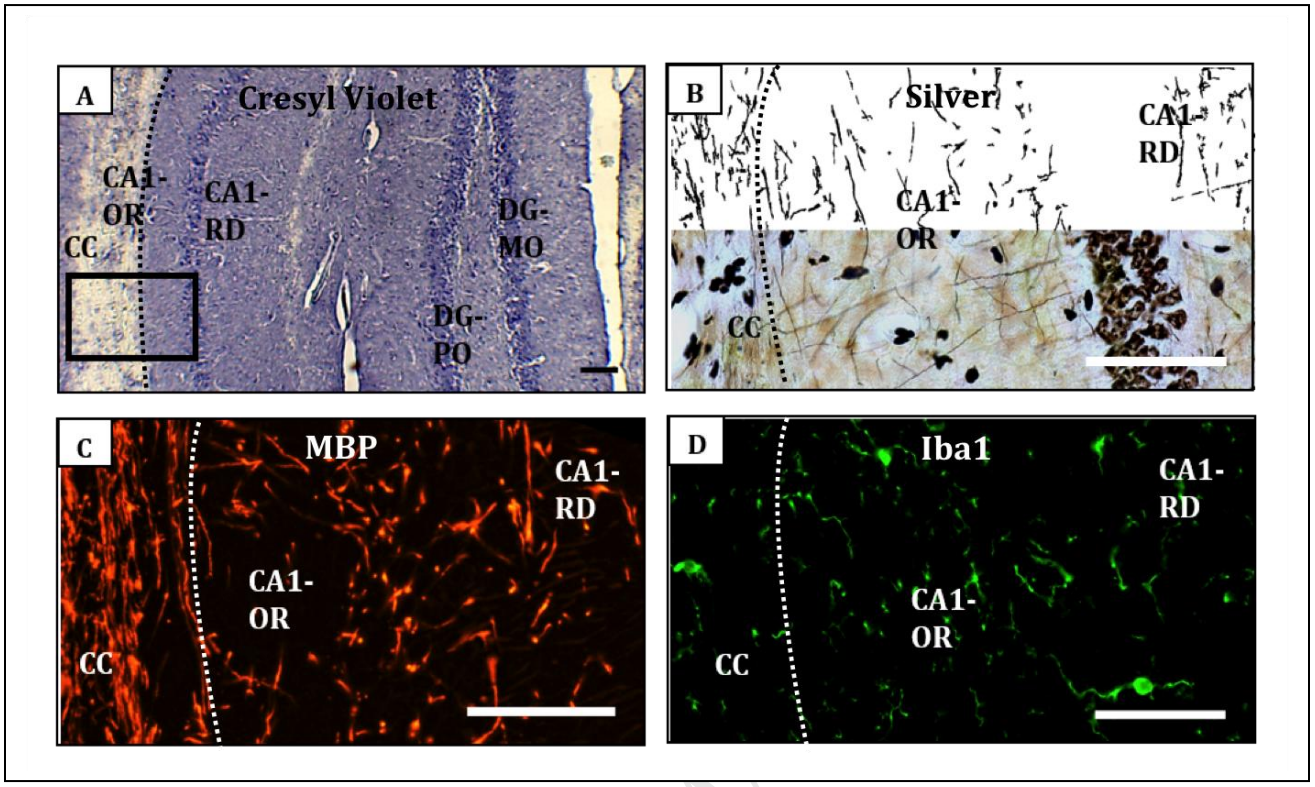

Figure 3: Histochemistry illustrating regions and stains. A, Cresyl violet stain, corpus callosum (CC) and dorsal hippocampus: CA1 subfields stratum oriens (approximate area of analysis 25 mm^2) and stratum radiatum (45 mm^2), dentate gyrus (DG) subfields molecular layer (90 mm^2) and polymorphic layer (15 mm^2). Black box outlines the regions shown in other panels. B, Silver stain; C, Myelin basic protein; D, Iba1. Scale bar, 100 µm.

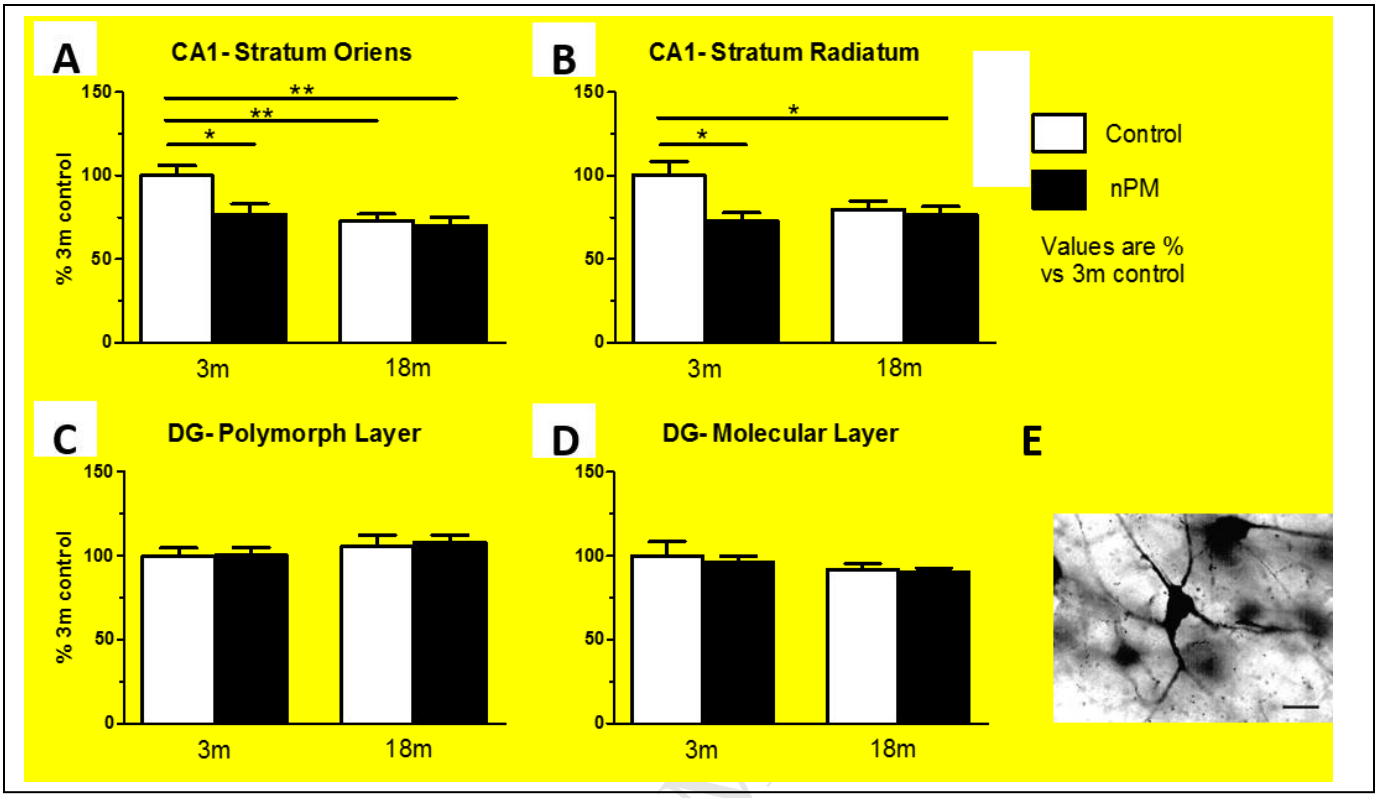

Figure 4: Hippocampus neurite area as total silver stained area per field (See Fig. 3).
A, Stratum oriens of CA1. nPM exposure in 3m mice decreased processes by 25% ($p<0.05$, ANOVA). 18m animals had equivalent decrease ($p<0.05$, ANOVA). No response to nPM in 18m mice.
B, Stratum radiatum of CA1. nPM exposure decreased processes by 25% ($p<0.05$, ANOVA). No baseline age changes.
C, Polymorphic layer of the DG. No change observed. D, Molecular layer of the DG. No change observed. E, Example of silver stained CA1 stratum radiatum neuron. Mean +/- SEM; N=9 per treatment. Scale bar 25 µm.

801

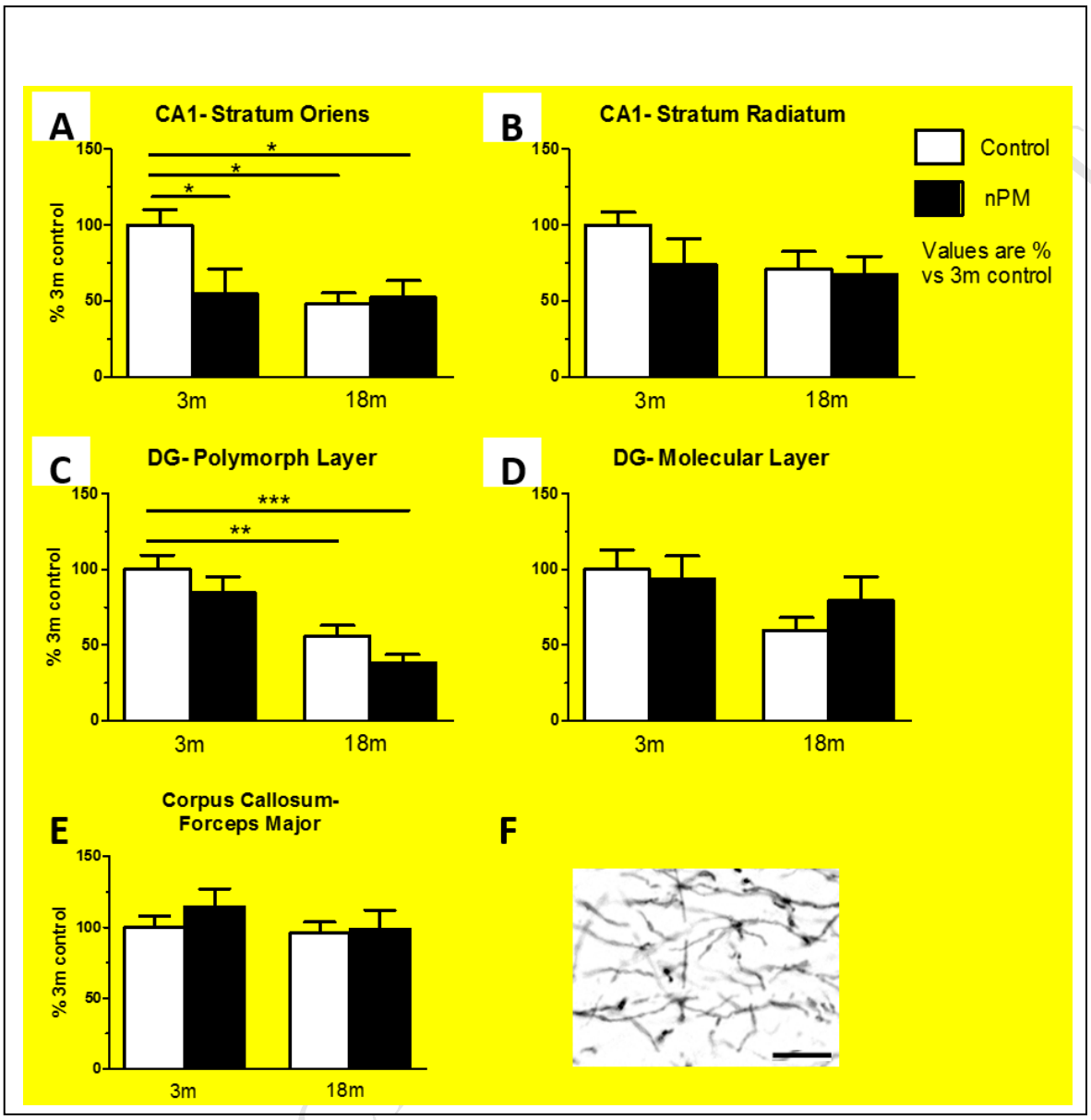

802

803 **Figure 5**: White matter immunohistochemistry for myelin basic protein in
804 hippocampus and corpus callosum (See Fig. 3). A, Stratum oriens of CA1. nPM
805 exposure in 3m mice decreased MBP by 50% ($p<0.05$, ANOVA). 18m animals
806 had equivalent decrease ($p<0.05$, ANOVA). No response to nPM in 18m mice.
807 B, Stratum radiatum of CA1. No change observed by age or nPM.
808 C, Polymorphic layer of the dentate gyrus (DG). No response to nPM in 3m or
809 18m mice. Baseline age change of 50% ($p<0.05$, ANOVA). D, Molecular layer of
810 the DG. No change observed. E, Forceps major of the corpus callosum. No
811 change observed. F, Example of MBP stained myelin in CA1 stratum radiatum.
812 Mean +/- SEM; N=9 per treatment. Scale bar 10 µm.
813

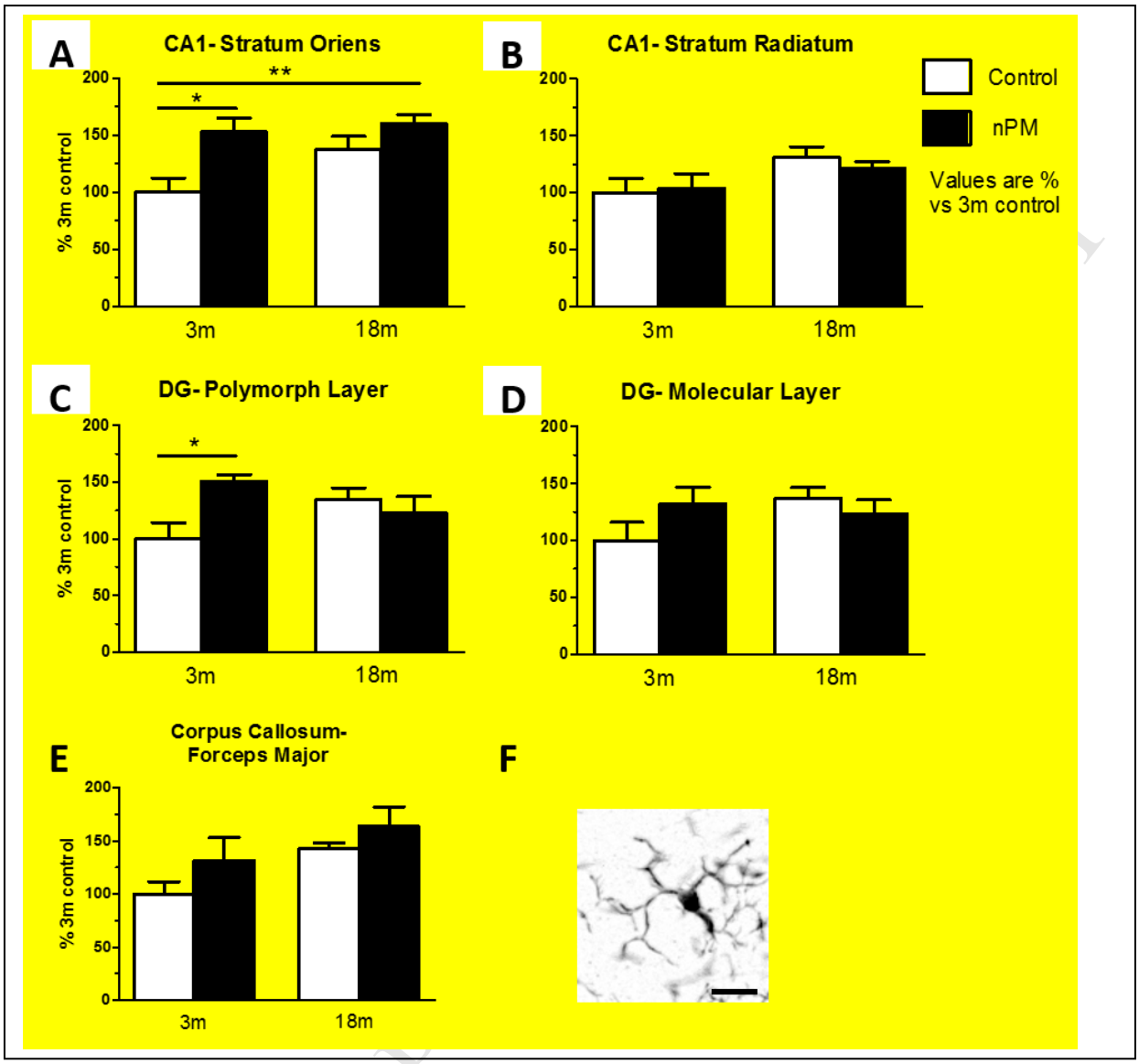

Figure 6: Microglial activation, measured by Iba1 immunohistochemistry (IHC), in regions of the hippocampus and corpus callosum (See Fig. 3). A, Stratum oriens of CA1. nPM exposure in 3m mice increased Iba1 by 50% ($p<0.05$, ANOVA). Older control mice showed a trend toward decrease, with no change observed by ANOVA, but $p<0.05$ by two-tailed t-test. No response to nPM in 18m mice. B, Stratum radiatum of CA1. No changes observed. C, Polymorphic layer of the dentate gyrus (DG). nPM exposure in 3m mice increased Iba1 by 50% ($p<0.05$, ANOVA). No baseline age changes or response to nPM in 18m mice observed. D, Molecular layer of the DG. No changes observed. E, Microglial expression in the corpus callosum, no change. F, Example of Iba1-stained microglial cell from CA1 stratum radiatum. Mean +/- SEM; N=9 per treatment. Scale bar 10 µm.

828

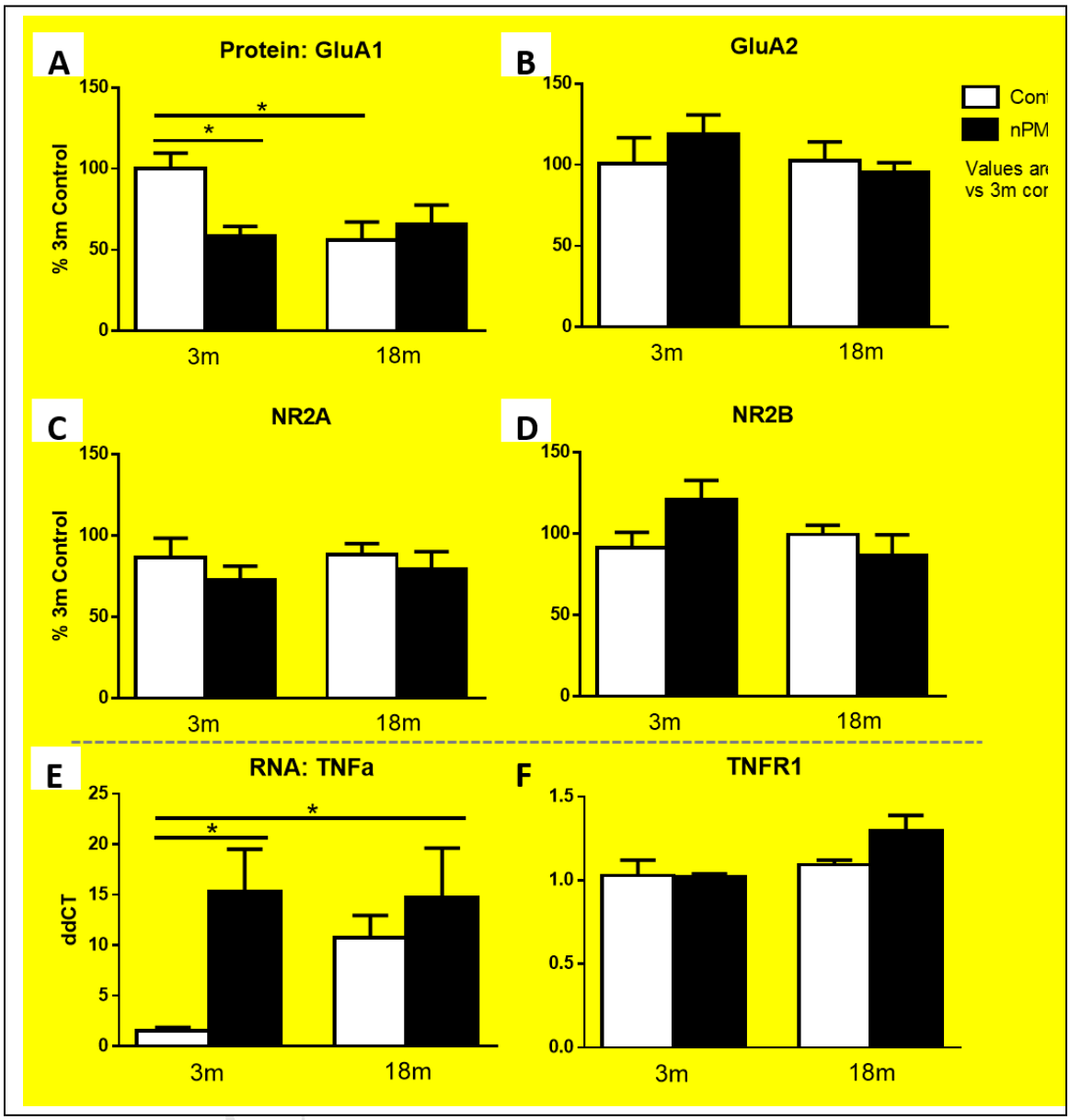

829 **Figure 7:** Protein concentration of glutamate receptor subunits from hippocampal
830 lysates. A, GluA1 protein was decreased 50% in the 3m mice by nPM exposure
831 ($p<0.05$, ANOVA). Baseline age decrease of 50% was observed ($p<0.05$,
832 ANOVA), with no effect of nPM in older mice. B, GluA2 protein showed no
833 change by age or treatment. C, NR2A showed no change by age or treatment. D,
834 NR2B showed no change. E, TNFa mRNA in the hippocampus, by q-PCR. nPM
835 exposure increased TNFa mRNA in young mice by 10x ($p<0.05$, ANOVA). Non-
836 exposed controls showed a trend for age increase that was not significant (P =
837 0.XX) because of individual variability. F, TNFR1 mRNA, no change by age or
838 treatment. Dotted line separates protein and RNA results. Mean +/- SEM; N=9
839 per treatment.

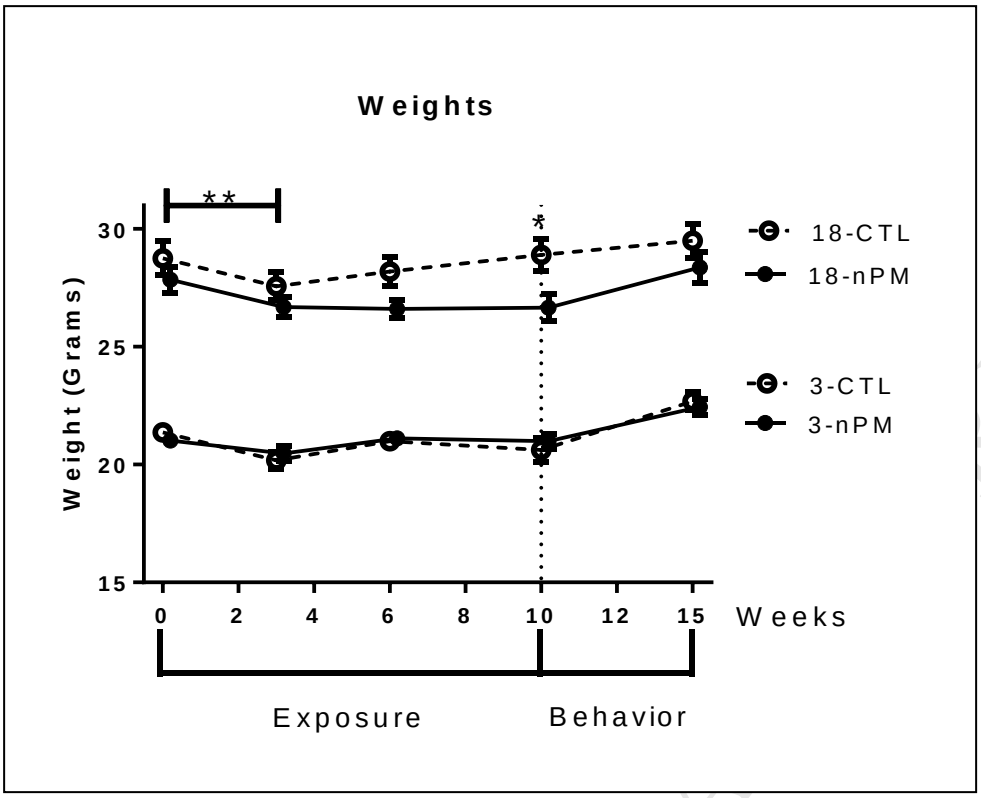

Figure 8: Body weight throughout exposure and 1 m post exposure. All groups showed initial weight loss ($p<0.01$, two-way ANOVA). All young mice and older controls recovered weight during the exposure, unlike older exposed mice; difference post exposure ($p<0.05$, one-way ANOVA). Older exposed mice recovered weight 1 m post exposure. Mean +/- SEM; N=9 per group.

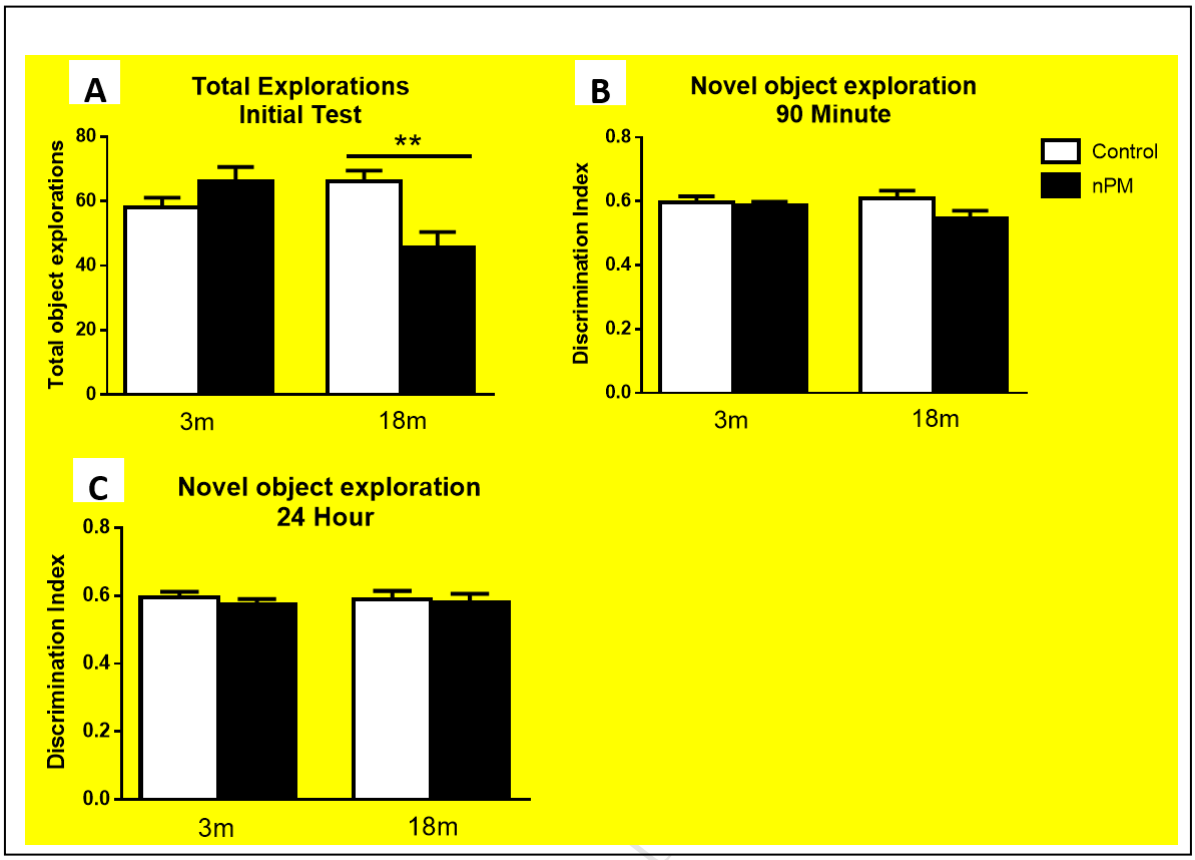

Figure 9: Novel Object Recognition (NOR) test, activity and discrimination index. A, Total number of explorations during the initial test. Older nPM exposed mice had reduced exploratory activity ($p<0.01$, one-way ANOVA). B, Discrimination index (exploration of novel object divided by total exploration) for the 90-minute posttest (short-term memory). C, Discrimination index for the 24-hour posttest (long-term memory). Mean +/- SEM; N=9 per treatment.

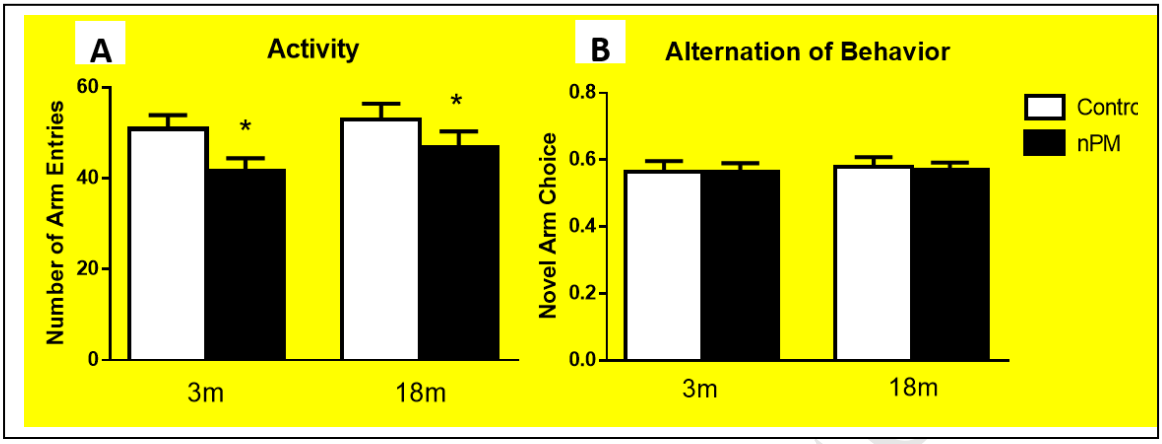

Figure 10: Spontaneous Alternation of Behavior (SAB) test. A, Total number of alternations between the three arms. Both ages showed effect of nPM ($p<0.05$, two-way ANOVA) B, Alternation of behavior (ratio of optimal arm choices). Mean +/- SEM; N=9 per treatment.

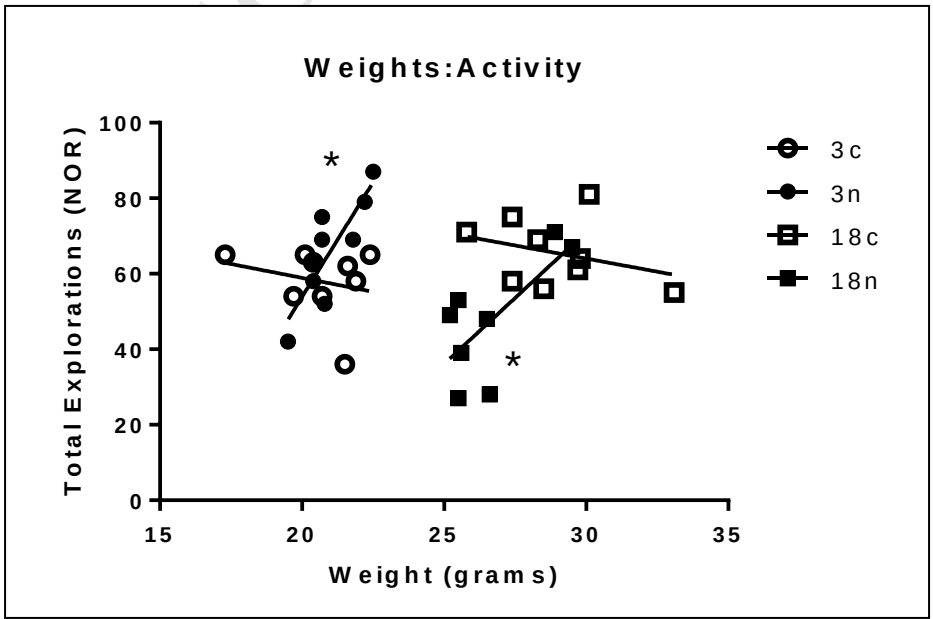

Figure 11: Correlations of body weight at the end of nPM exposure vs total number of explorations in the initial NOR test. Both ages showed effect of nPM (r=0.5076).

Table 1: Summary of age differences in control mice, not nPM exposed.

Age Differences				
Region		**Neurites**	**Myelin**	**Microglial Activation**
CA1	Oriens	-25%	-50%	+35%
	Radiatum	0	0	0
DG	Polymorph	0	-45%	0
	Molecular	0	0	0
Corpus Callosum		NA	0	0

Summary of age differences in control mice (Figures 4,5,6). 0, no change, “Inc” denotes an increase versus young control, “Dec”, a decrease versus young control, and NA, not measured.

Treatment Differences				
Region		**Neurites**	**Myelin**	**Microglial Activation**
CA1	Oriens	-25%	-45%	+50%
	Radiatum	-25%	0	0
DG	Polymorph	0	0	+50%
	Molecular	0	0	0
Corpus Callosum		NA	0	0

Table 2: Summary of treatment differences in young animals. Values are versus young control air mice. 0 denotes no change, “Inc“ denotes increase, “Dec” shows a decrease, and NA means not measured. CA1- cornus ammonis 1, DG- dentate gyrus.

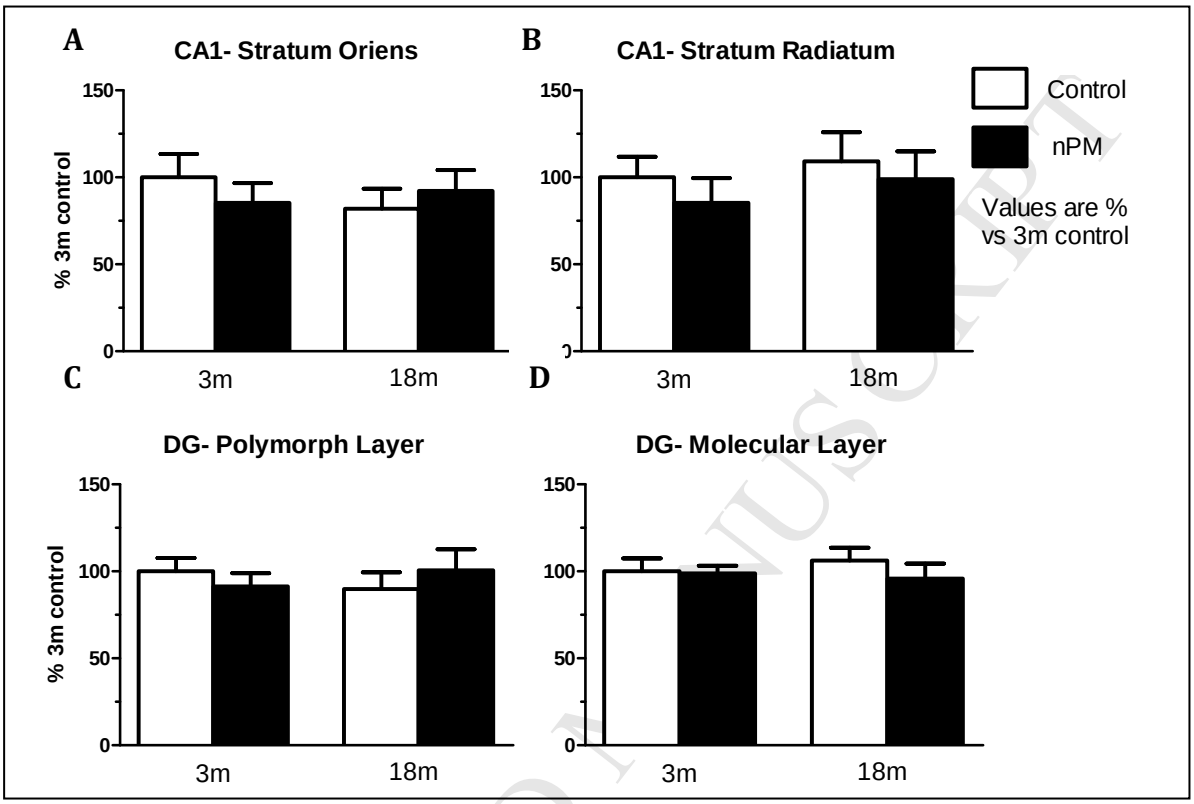

Supplementary Figure 1: Neuronal perikarya, visualized by silver staining, in regions of the hippocampus and corpus callosum. No changes observed for any region. A) Stratum oriens of the cornus ammonis 1 (CA1). B) Stratum radiatum of the CA1. C) Polymorphic layer of the dentate gyrus (DG). D) Molecular layer of the DG.

- Age response to traffic-related air pollution exposure is investigated
- Young mice show neurite and myelin loss in the CA1 resembling age changes
- Older mice demonstrate an age-ceiling effect, and do not respond to exposure